A. Ghoggal
S. E. Zouzou
A. Aboubou
M. Sahraoui

J. Electrical Systems 1-4 (2005): 69-82

Regular paper

A 2D Model of Induction Machine Dedicated to faults Detection : Extension of the Modified Winding Function

This paper deals mainly with the modeling of induction machine inductances by taking into account all the space harmonics, the skewing rotor bars effects and linear rise of MMF across the slot. The model is established initially in the case of symmetric machine, which corresponds to the case of a constant air-gap, then in the other case where the machine presents a static or dynamic, axial or radial eccentricity. This objective would be achieved by exploiting an extension in 2-D of the modified winding function approach (*MWFA*).

Keywords: Induction machines, inductance, MWFA, spaces harmonics, skew.

1. INTRODUCTION

The multiple coupled circuit, defined in the aim of approaching the real structure of the rotor cage, supposes that this one gathers a number of loops forming a polyphase winding, each loop consists of two adjacent bars and the two portions of the end ring which connect them [1]. Such a structure was used with profit in the diagnosis of the induction machine. Several studies were carried out in this axis, and made possible to reveal some phenomena rising from a defect, such as appearance of higher or lower side-band frequencies than the stator frequency in the spectral analysis of the line currents, torque, speed and power. Some papers supposes a perfect distribution of the MMF in the air-gap, others adopt models taking into account the real distribution of machine's windings [2], in particular with the implication of winding function, then, MWFA [3], where it is possible to detect some phenomena accompanying a probable eccentricity, and finally, the introduction of the axial dimension [4],[5]. The model is thus ready to define inductances of a machine taking into account the skew of the slots, and which can be extended to the study of other types of axial asymmetries, namely, the axial eccentricities.

In this work, a 2-D model of the induction machine will be approached while focusing the study on its first aim; the modeling of induction machine with non-sinusoidal distribution of the stator winding, and non-uniformity of the air gap. Simulation results as well as comments will be exposed.

Corresponding author: ghoetudes@yahoo.fr
Laboratoire de Génie Electrique, Département d'Electrotechnique,
Université Mohamed Khider B P. 145, Biskra - Algérie.

2. A 2-D PRESENTATION OF THE MODIFIED WINDING FUNCTION APPROACH

To formulate the problem, we refer to Figure. 1 which gathers two cylindrical masses separated by an air-gap, one of them hollow and represents the stator, and the other represents the rotor. An *abcda* arbitrary path is defined thanks to a reference frame fixed on the stator, to an axial reference and to the mechanical position of the rotor measured by respecting a fixed stator reference. At a rotor position θ_r, and at $\varphi_0 = 0$ and $z_0 = 0$ are the points a and *b*, and at φ and z are *c and d*. On another side, *a* and *d* are located on the stator inner surface, and *b* and c on the rotor external surface.

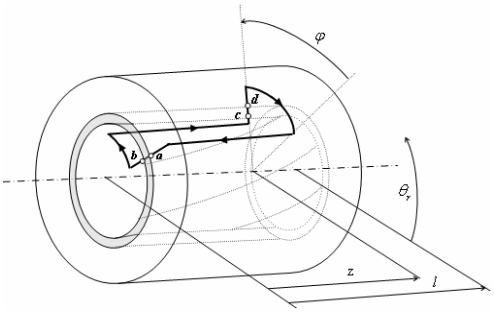

Figure 1: Elementary induction machine.

Let us take again the same stages of [3] but with the use of the axial dimension. Thus, according to the Gauss's law, the integral of the magnetic flux density on closed surface S of a cylindrical volume defined in comparison to the average radius of the air-gap *r* is null:

$$\oint_s B \; ds = 0 \tag{1}$$

By defining, at any of coordinates (φ, z), the magnetic field intensity H, the magnetomotrice force *F* and the effective air-gap function g, such as $B = \mu_0 H$ and $H = F / g$, in this case (1) become

$$\mu_0 r \int_0^{2\pi} \int_0^{l} \frac{F(\varphi, z, \theta_r)}{g(\varphi, z, \theta_r)} dz d\varphi = 0 \tag{2}$$

where *l* is the effective length of the air-gap. On the other side, and according to the Ampere's law, it is possible to write

$$\oint_{abcda} H(\varphi, z, \theta_r) dl = \int_{\Omega} J ds \tag{3}$$

where Ω is a surface enclosed by the closed path *abcda*, and *J* the current density. According to the MMF and the number of turns enclosed by the closed path *abcda* and traversed by the same current *i* , (3) can be written as

$$F_{ab}(0,0,\theta_r) + F_{bc} + F_{cd}(\varphi, z, \theta_r) + F_{da} = n(\varphi, z, \theta_r) i \tag{4}$$

where $n(\varphi, z, \theta_r)$ is called the 2-D spatial winding distribution [5], or the 2-D turns function.

By considering an infinite permeability of iron, F_{bc} and F_{da} are null, the substitution of these values in (4) gives

$$F_{cd}(\varphi, z, \theta_r) = n(\varphi, z, \theta_r) i - F_{ab}(0,0,\theta_r) \tag{5}$$

By introducing the average value of the inverse air-gap function $\langle g^{-1}(\varphi, z, \theta_r)\rangle$ given by

$$\langle g^{-1}(\varphi, z, \theta_r)\rangle = \frac{1}{2\pi}\int_0^{2\pi}\left[\frac{1}{l}\int_0^{l} g^{-1}(\varphi, z, \theta_r) dz\right] d\varphi \tag{6}$$

and while exploiting (2) and (5), it will be possible to lead to the expression giving $F_{cd}(\varphi, z, \theta_r)$ as follows:

$$F_{cd}(\varphi, z, \theta_r) = n(\varphi, z, \theta_r) i - \frac{1}{2\pi\, l\langle g^{-1}(\varphi, z, \theta_r)\rangle}\int_0^{2\pi}\int_0^{l} n(\varphi, z, \theta_r) g^{-1}(\varphi, z, \theta_r) i\, dz\, d\varphi \tag{7}$$

The 2-D winding function can be obtained by dividing the members of (7) by *i*:

$$N(\varphi, z, \theta_r) = n(\varphi, z, \theta_r) - \frac{1}{2\pi\, l\langle g^{-1}(\varphi, z, \theta_r)\rangle}\int_0^{2\pi}\int_0^{l} n(\varphi, z, \theta_r) g^{-1}(\varphi, z, \theta_r) dz\, d\varphi \tag{8}$$

It is to be noticed that this new expression does not hold any restriction as for the axial uniformity, particularly in term of skewing slots and axial non uniformity of the air-gap.

3. CALCULATION OF INDUCTANCES

3.1 Machine with uniform air-gap

Firstly, supposing that the machine is symmetrical. The air-gap length g is reduced to g_0 which is the radial air-gap length in the case of no eccentricity. If *F* is the MMF distribution in the air-gap due to the current i_{A_1} flowing in an

arbitrary coil A_i, and knowing that the elementary flux corresponding in the air-gap is measured in comparison to an elementary volume of section *ds* and length g_0 such as

$$d\phi = \mu_0 F g_0^{-1} ds \tag{9}$$

the calculation of total flux returns to a calculation of double integral. By carrying out the change of variable $x = r\varphi$ and $x_r = r\theta_r$ the study is transformed to a reference with axes X and Z where we can imagine a plane representation of the machine. It is clear that, in this case, *x* translate correctly the linear displacement along the arc corresponding to the angular opening φ. It is the same thing concerning x_r and θ_r.

Knowing that N is the MMF per unit of current, the expression giving the flux seen by all the turns of coil B_j of winding *B* due to i_{Ai} flowing in coil A_i will be reduced as

$$\phi_{BjAi} = \frac{\mu_0}{g_0} \int_{x_{1j}}^{x_{2j}} \int_{z_{1j}(x)}^{z_{2j}(x)} N_{Ai}(x,z,x_r) n_{Bj}(x,z,x_r) i_{Ai} dz dx. \tag{10}$$

This is due to the fact that by taking into account the axial asymmetry $n_{Bj}(x,z,x_r)$ will be defined so as to be able to translate the skew of the slots. In 2-D, it will be written in the following way:

$$n_{Bj}(x,z,x_r) = \begin{cases} w_{Bj} & x_{1j} \langle x \langle x_{2j} \quad , \quad z_{1j}(x) \langle \ z(x) \ \langle z_{2j}(x) \\ 0 & \text{in the remaining interval} \end{cases} \tag{11}$$

where w_{Bj} is the number of turns of coil B_j. It is equal to 1 in the case of a rotor loop. Generally, the total flux ψ_{BA} related to all coils composing winding A and *B*, holds its general expression by integrating over the whole surface. Then knowing that the mutual inductance L_{BA} is the flux ψ_{BA} per unit of current, yields

$$L_{BA}(x_r) = \frac{\mu_0}{g_0} \int_0^{2\pi r} \int_0^{l} N_A(x,z,x_r) n_B(x,z,x_r) dz dx \tag{12}$$

Note that a rearrangement of (12) makes possible to define an inductance per unit of length as described in [4]:

$$L_{BA}(x_r) = \int_0^{l} L'_{BA}(z,x_r) dz \tag{13}$$

In the same way as [1], and according to the manner of connecting the coils translated by the sign in (14), this inductance can be obtained by summing all mutual inductances between the *q* and *p* coils of windings *A* and *B* respectively, such as:

$$L_{BA}(x_r) = \sum_{i=1}^{q}\sum_{j=1}^{p} \pm L_{B_j A_i}(x_r) \qquad (14)$$

3.2 Bars skewing

Figure. 2 depicts the passage of a rotor loop r_j under the field of a stator coil A_i. The skew is translated by the definition of z(x) in (10) which *will* be a function describing the uniform skew, or particularly, the case of spiral skew.

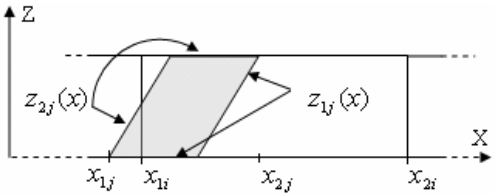

Figure 2: Representation of the skew.

Note that the pitch α_{Ai} of the coil A_i is defined in comparison to its sides placed at $x_{1i} = r.\varphi_{1i}$ and $x_{2i} = r.\varphi_{2i}$, and that the effect of linear rise of MMF across the slot is not represented in the Figure.

3.3 Slot opening

Let us examine the case of coil A_i with w_{Ai} turns placed in slots which, according to cases, can present an opening of width β according to the considered configuration. Figure. 3 shows the turns function of coil A_i if the slot opening is taken into account in the calculation of the resultant linear rise of MMF across the slot.

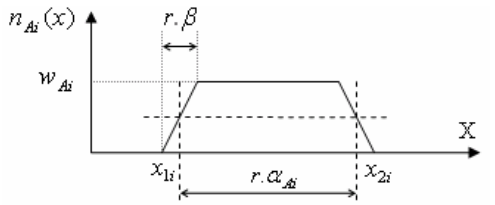

Figure 3: Turns function of coil A_i.

3.4 Machine with an eccentric rotor

Equation (12) takes its generalized form as:

$$L_{BA}(x_r) = \mu_0 \int_0^{2\pi r} \int_0^{l} N_A(x,z,x_r) n_B(x,z,x_r) g^{-1}(x,z,x_r) dz dx. \quad (15)$$

With the use of (14) and (15), it will be possible to calculate all inductances of the machine if:

Case of a purely radial eccentricity: $g^{-1} = g^{-1}(x, x_r)$.

The case where this eccentricity appears also along the Z axis:
$g^{-1} = g^{-1}(x, z, x_r)$.

The general expression of g^{-1} is given by

$$g^{-1}(x,z,x_r) = \frac{1}{g_0(1-\delta_s(z)\cos(x/r) - \delta_d(z)\cos((x-x_r)/r)} \quad (16)$$

where δ_s and δ_d are the amounts of static and dynamic eccentricity respectively which are function of z. A numerical calculation makes possible to find the integral (15), however, an analytical resolution call upon an approximated expression of g^{-1} by carrying out a development in Fourier series. A good result would be obtained while stopping at the third term, such as:

$$g^{-1}(x,z,x_r) \approx P_0(z) + P_1(z)\cos(x/r - \rho) + P_2(z)\cos(2(x/r - \rho)) \quad (17)$$

with ρ , P_0, P_1 and P_2 are calculated from g_0 , $\delta_s(z)$, $\delta_d(z)$ and θ_r which were described in [7] and [8]. It is to be recalled that for any windings *A* and *B*, equality $L_{AB} = L_{BA}$ is always checked [7], and that all were calculated compared to an average radius of the air-gap r in the case of no eccentricity, while admitting that the variations in the radius of the air-gap R due to the eccentricity are negligible in front of the radius itself, which is not the case concerning g , it is what can be translated as

$$\frac{R(x,z,x_r)}{g(x,z,x_r)} = \frac{r \pm \Delta R(x,z,x_r)}{g_0 \pm \Delta g(x,z,x_r)} \approx \frac{r}{g_0 \pm \Delta g(x,z,x_r)} \quad (18)$$

4. SIMULATION RESULTS

4.1 Machine with uniform air-gap

The first induction machine studied in this paper is a three-phases, 4-poles motor [4], whose parameters appear in the Appendix, and the structure of the stator coils of Figure. 4, where only phase A is represented, and one of its coils numbered. Each circle represents the section of an elementary coil of *w* turns. A, B, and C are the three stator phases, and r_j the j^{th} rotor loop.

Figure 4: Winding of stator phase A.

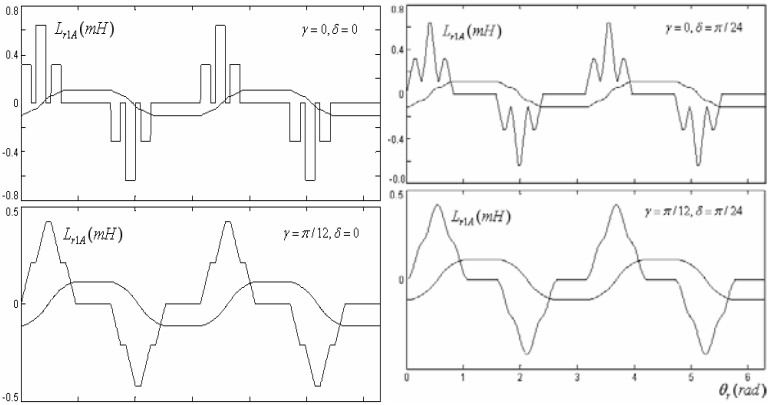

Figure 5: Mutual inductance between stator phase A and rotor loop r_1.

Figure. 5 illustrates the functions which describe the mutual inductances L_{r1A} between the first stator phase A, and the first rotor loop, in the four cases considered, without and with taking into account the slots opening and the skewing of rotor bares. A rotor loop is regarded as being a coil with one turn. Note that the mutual inductance between phase and the second rotor loop is the same as it was given in Figure. 5, but shifted to the left by $2\pi/Nb$. As for the other inductances, L_{r1B} and L_{r1C} are identically reproduced, but shifted to the right by $\pi/3$. The mechanical angle of skewing of the rotor bars is $\gamma=\pi/12$ rad, which is selected equal to one stator slot pitch [6], and the width of slot opening $\beta=\pi/24$. In each figure, the function whose maximum value is most significant represents the first derivative of the curve of mutual inductance L_{r1A}.

As for the self and the mutual inductances between windings of the same frame (stator or rotor), it should be noticed that those are not affected by the effect of skewing, however, a variation in the values of the stator inductances is noticed, and it is due to the taking into account of the linear rise of MMF across the slot (Table I).

Table I: stator Inductances

β	L_A (H)	L_{AB} (H)
0	0.1198	-0.0532
π/24	0.1165	-0.0529

4.2 Machine with an eccentric rotor

1. *Radial eccentricity*

The second specific induction motor studied is a three-phases, 11kw, 50Hz, 4-poles motor, having four coils per phase group, eight coils per phase, series connected [10]. The others parameters are given in the Appendix. Figure. 6-11 show the simulation results for different degrees of eccentricity, and with three terms P_0, P_1 and P_2 used in the development of g^{-1}.

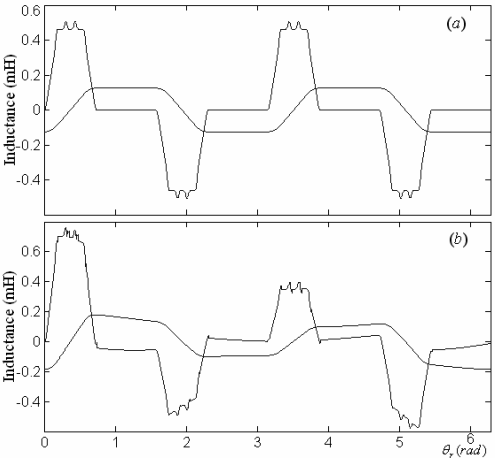

Figure 6: L_{r1A} and $dL_{r1A}/d\theta_r$ a) symmetric machine, b) δ_s =35%, δ_d =0.

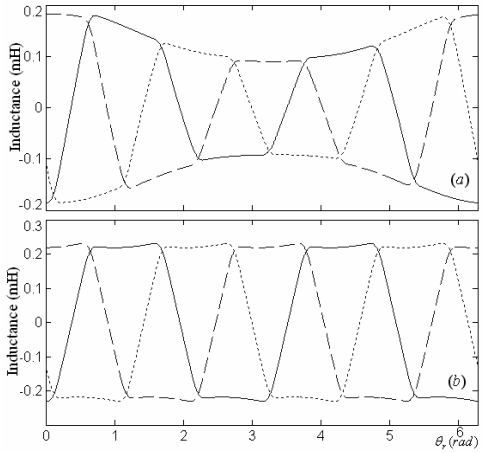

Figure 7: Mutual inductances $L_{r1A}, L_{r1B}, L_{r1C}$. a) δ_s =35%, δ_d =0 b) δ_s =0%, δ_d =50%.

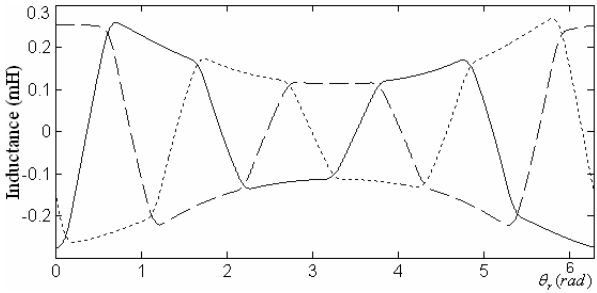

Figure 8: $L_{r1A}, L_{r1B}, L_{r1C}$ case of mixed eccentricity of δ_s = 35% and δ_d = 25%.

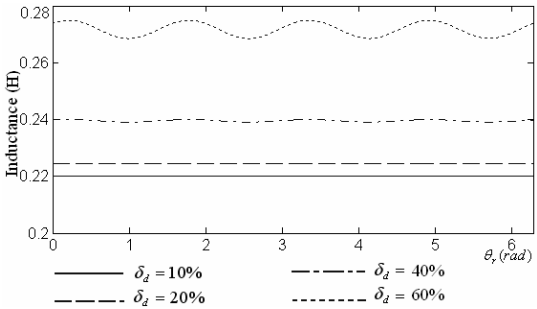

Figure 9: Self inductance of phase A for different degrees of dynamic eccentricity.

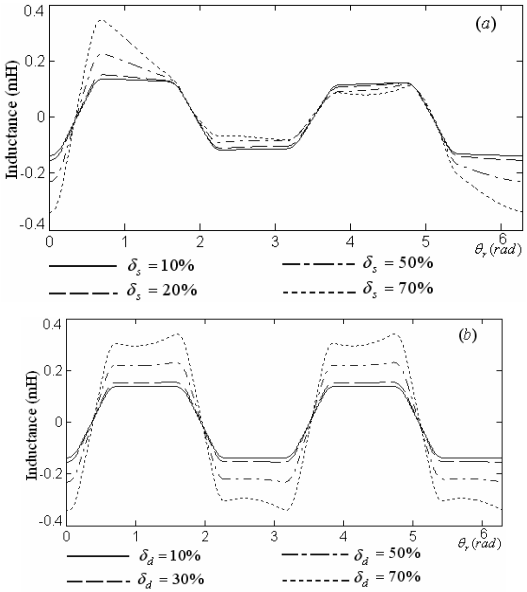

Figure 11: Mutual inductance L_{r1A} for different degrees of eccentricity, a) Static eccentricity, b) Dynamic eccentricity.

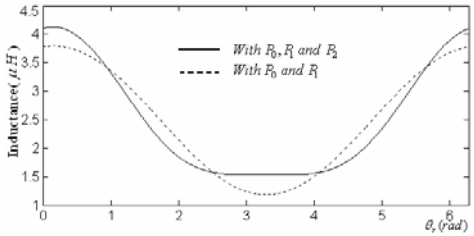

Figure 10: Self inductance of rotor loop r_1 for 50% of static eccentricity.

2. *Axial eccentricity*

To examine the case of the static eccentricity, the expression of $\delta_s(z)$ must be defined. According to Figure. 12 showing the external diameter of the rotor and the internal diameter of the stator with exaggeration in the representation of the air-gap, $\delta_s(z)$ can be written as

$$\delta_s(z) = \delta_{s0}(1 - z/L) \tag{19}$$

Like presented in Figure. 12, the minimum air-gap for $z = 0$ is supposed at $\varphi = 0$ along the vertical axis. The minimal air-gap has a fixed angular position for the different values of z inferior than L, but its value depends on z.

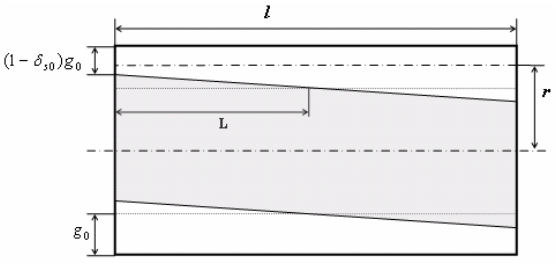

Figure 12: Illustration of the axial eccentricity.

On another side, if the perfectly concentric section of the rotor corresponds to $z = L$, in this case, in the modeling of the eccentricity, L must be selected superior than a certain value guaranteeing the existence of an air-gap with $g(x, z, x_r) \neq 0$ along the rotor length. For $L \to +\infty$, as a result $\delta_s(z) \to \delta_{s0}$, and the study returns to the case of the purely radial eccentricity. Figure. 13 chows the mutual inductance between stator phase A and the first rotor loop with rotor position when $\delta_{s0} = 70\%$ and $L = l/2$.

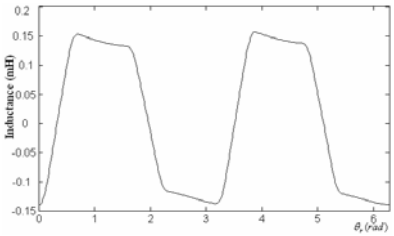

Figure 13: L_{r1A} for $\delta_{s0} = 70\%$ and $L = l/2$.

4.3 Operation under condition of mixed eccentricity

Knowing that the cage can be viewed as identical and equally spaced rotor loops, it is possible to establish voltage equations of stator and rotor loops as [1- 2]:

$$[U_s] = [R_s]\ [I_s] + \frac{d[\psi_s]}{dt} \tag{20}$$

$$[\ 0\ ] = [R_r]\ [I_r] + \frac{d[\psi_r]}{dt} \tag{21}$$

$$[\psi_s]=[L_{ss}]\ [I_s]+[L_{sr}]\ [I_r] \tag{22}$$

$$[\psi_r]=[L_{rs}]\ [I_s]+[L_{rr}]\ [I_r] \tag{23}$$

The vector $[U_s]$ corresponds to the stator voltages, $[I_s]$ and $[I_r]$ to the stator and rotor currents. *m* is the number of stator phases and N_b the number of rotor bars. $[R_s]$ is an *m* dimensional diagonal matrix, $[L_{ss}]$ is an $m\times m$ symmetric matrix, $[L_{sr}]$ is an $m\times(N_b+1)$ matrix, and $[R_r]$ and $[L_{rr}]$ are $(N_b+1)\times(N_b+1)$ matrix.

Adding to the above equations the mechanical and electromagnetic torque equations:

$$C_e-C_r=J_r\frac{d\omega_r}{dt},\ C_e=\left(\frac{dW_{co}}{d\theta_r}\right)\Bigg|_{(I_s,I_r=\text{constant})} \tag{24}$$

$$\begin{aligned}W_{co}=\frac{1}{2}\Big([I_s]^T[L_{ss}]\ [I_s]+[I_s]^T[L_{sr}]\ [I_r]\\ +[I_r]^T[L_{rr}]\ [I_r]+[I_r]^T[L_{rs}]\ [I_s]\Big)\end{aligned} \tag{25}$$

where W_{co} is the co-energy, C_e the electromagnetic torque, C_r the load torque, J_r the rotor load inertia, and ω_r the mechanical speed of the rotor. Figure. 14 shows the simulation result of the operation of machine (2) under conditions of mixed eccentricity of $\delta_s = 40\%$, $\delta_d = 20\%$.

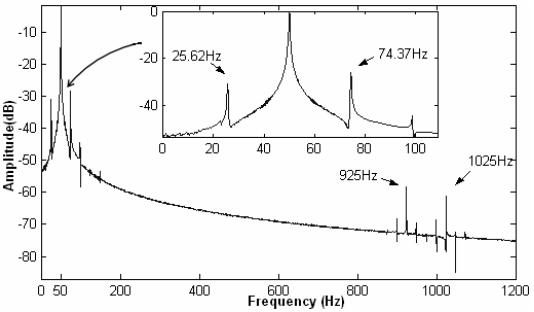

Figure 14: Stator current spectra with mixed eccentricity condition, δ_s =40%, δ_d =20%, slip =2.5%.

In the spectra of Figure. 14 relating to the current of the first stator phase, it is possible to see the first components which are function of static eccentricity. This result is derived from the general equation given in [8], and described by

$$f_{slot+ecc} = f_s \cdot (\frac{N_b}{p}(1-s) \pm 1) \tag{26}$$

where f_s represents the mains frequency and *s* the slip. In the zoom appear the low frequency components near the fundamental. This result is as predicted in [9] and described by

$$f_{ecc} = f_s \cdot (1 \pm (1-s)/p) \tag{27}$$

5. CONCLUSION

In this work, the bases of MWFA were presented with introduction of the axial dimension. It was applied in the calculation of the induction machine inductances with, initially, taking into account of all the space harmonics. And secondly, taking into account of the effects generated by the skew and linear rise of MMF across the slots. Then finally, the modeling in the air gap eccentricity conditions, in the different cases of eccentricity considered static, dynamic, radial and axial eccentricity. For that, a simulation tools was established. The obtained results were compared with the final results of [4] and [10], and a perfect agreement was noticed, but this new technique prove less complicated to be translated into algorithm than that given by the expression of inductance per unit of length as described in [4]. It is advisable to integrate the effect of saturation, and to envisage operation under other faults conditions. It is what constitutes our work perspective.

APPENDIX: Machines Parameters

- Machine 1:

$g_0 = 0.0006m$, $r = 0.066m$, $l = 0.115m$, $w = 20$, *Nb* =36, *Ne*=24.

- Machine 2:

$g_0 = 0.0008m$, $r = 0.082m$, $l = 0.11m$, $w = 28$, *Nb*=40, *Ne*=48, L_b =95*nH*, L_e =18*nH*, $R_s = 1.75\Omega$, $R_b = 31\mu\Omega$, $R_e = 2.2\mu\Omega$, $J_r = 0.0754kgm^2$, $\gamma = \pi/20rad$, $\beta = \pi/86rad$.

REFERENCES

[1] X. Luo, Y. Liao, H.A. Toliyat, A. El-Antably, and T.A. Lipo, Multiple coupled circuit modeling of induction machines, IEEE Trans. Industry Applications, vol. 31, no. 2, pp. 311-318, Mar./Apr. 1995.

[2] H. A Toliyat, T.A Lipo, Transient analyze of induction machines under stator, rotor bar and end ring faults, IEEE Trans. Energy Conv, vol. 10, no. 2, pp. 241-247, June 1995.

[3] N. A. Al-Nuaim and H.A. Toliyat, A novel method for modeling dynamic air-gap eccentricity in synchronous machines based on modified winding function theory, IEEE Trans. Energy Conv, vol. 13, no. 2, pp. 156-162, June 1998.

[4] M. G. Joksimovic, D. M. Durovic and A. B. Obradovic, Skew and linear rise of MMF across slot modeling-Winding function approach, IEEE Trans. Energy Conversion, Vol. 14, no. 3, pp. 315-320, Sept. 1999.

[5] G. Bossio, C.D. Angelo, J. Solsona, G. García and M. I. Valla, A 2-D Model of the induction machine: Extension of the modified winding function approach, IEEE Trans. Energy Conversion, vol. 19, no. 1, pp. 144-150, Mar. 2004.

[6] M. Liwschitz and L. Maret, Calcul des machines électriques, Bibliothèque de l'ingénieur, Editions SPES Lausanne: 1970.

[7] J. Faiz and I. Tabatabaei, Extension of winding function theory for non-uniform air gap in electric machinery, IEEE Trans. Magnetics, vol. 38, no. 6, pp. 3654-3657, Nov. 2002.

[8] S. Nandi, R.M. Bharadwaj and H.A. Toliyat, Performance analyze of three-phase induction motor under mixed eccentricity condition, IEEE Trans. Energy Conversion, vol. 17, no. 3, pp. 392-399, Sept. 2002.

[9] D.G. Dorrell, W.T. Thomson and S. Roach, Analyze of air gap signals as function of combination static and dynamic air gap eccentricity in 3-phase induction motors, IEEE Trans. Industry Applications, vol. 33, no. 1, pp. 24-34, Jan./Feb. 1997.

[10] M. G. Joksimovic, D. M. Durovic, J. Penman and N. Arthur, Dynamic simulation of dynamic eccentricity in induction machines-Winding function approach, IEEE Trans. Energy Conversion, vol. 15, no. 2, pp. 143-148, June 2000.